



0017-9310(95)00025-9

Heat and mass transfer coupling between vaporizing droplets and turbulence using a Lagrangian approach

A. BERLEMONT, M. S. GRANCHER and G. GOUESBET

LESP-URA CNRS, 230 INSA de Rouen, BP 8 76131 Mont Saint Aignan Cedex, France

(Received 12 July 1994 and in final form 23 December 1994)

Abstract—A Lagrangian approach is developed for droplet vaporization in turbulent fields, with two-way coupling between phases. Specific source terms induced by phase changes are described and results are presented for methyl alcohol droplet vaporization in a heated turbulent round jet. A high coupling is observed between production and diffusion processes for the vapour mass fraction and fluid temperatures. Droplet diameter distributions are strongly dependent on the turbulent dispersion and droplet history.

INTRODUCTION

Numerous studies are currently devoted to studying the droplet vaporization phenomena and more generally the droplet combustion. Practical situations, such as industrial burners, diesel engines and more specifically rocket engines, involve two fluid phases which are almost invariably interacting with each other. Simulations of such two-phase flows appear quite complex since they must account for turbulent dispersion, phase changes and coupling between both processes.

Turbulent two-phase flow problems can be handled following two theoretical approaches: the Eulerian approach and the Lagrangian approach (Berlemont *et al.* [1]). In the Eulerian approach (Reeks [2], Elghobashi *et al.* [3], Picart *et al.* [4] among others), particle trajectory constructions and statistics are not explicitly carried out at a computational level, but are explicitly achieved at a conceptual level through equation closure assumptions, for instance by using a dispersion tensor (Gouesbet *et al.* [5], Desjonquères *et al.* [6]). The discrete character of the underlying process is thus modelled by a continuous description of the particle field. Although sophisticated Eulerian two-phase flow models have been developed (Simonin [7], Reeks [8]), closure assumptions are generating in most cases new constants, resulting possibly in a loss of generality. However unsteady situations are more easily solved through a Eulerian approach.

On the other hand, the Lagrangian approach allows one to account for the instantaneous flow properties encountered by the particles, and thus involves each particle history starting from its injection into the flow field. Moreover, the evolution of particle diameter distributions remains difficult to predict in a Eulerian scheme, but can be readily introduced in a Lagrangian approach.

From the detailed study of the evaporation of an

isolated droplet in a given flow field, models have been deduced to describe the droplet vaporization. These models involve the temperature and vapour mass fraction of the surrounding fluid, and the droplet relative velocity. For turbulent flows, these quantities are fluctuating along the particle trajectories and thus the droplet behaviour is strongly linked to its history from injection. The Lagrangian approach appears particularly well designed to study the influence of the turbulence on vaporizing droplets, when the Eulerian method would only deal with mean quantities.

Simulations have been first carried out for methyl alcohol droplets in grid turbulence (Berlemont *et al.* [9]) where particular attention has been paid to the respective influence of fluctuating temperatures, fluctuating vapour mass fractions and fluctuating velocities on mean diameter and diameter distributions of the droplets. An important result of the turbulence influence is the broadening of the diameter pdf which is coupled with the particle dispersion process. The broadening effect of diameter distributions then cannot be neglected, particularly when temperature fluctuations occur in the flow under study.

The aim of the present paper is to extend our model to turbulent jet applications, and to account for the two-way coupling between the fluid turbulence and the droplet heat transfers to discuss the interaction between vapour production and turbulent diffusion. In this paper the vaporization model and the particle tracking procedure are first recalled, then the two-way coupling source terms are detailed, and finally, simulations in a heated turbulent round jet are presented and the results are discussed.

VAPORIZATION MODEL

Vaporization models widely rely on the so-called “corrected spherical symmetry” hypothesis. In these

$$\frac{dT^s}{dt} = \frac{6}{D^2} \frac{\lambda}{\rho_1 C_1} \times \left[(T^\infty - T^s) Nu - \frac{L}{C_{\text{vap}}} \Lambda \right] \quad (5)$$

where C_1 is the specific heat of the liquid, T^∞ is the fluid temperature, L is the latent heat of vaporization, and Nu is the Nusselt number defined by:

$$Nu = \frac{\Lambda}{\exp(\Lambda/2) - 1} = \frac{q_g}{\frac{\lambda(T^\infty - T^s)}{D}} \quad (6)$$

where q_g is the heat flow rate on the droplet surface.

In order to account for the influence of convection on droplet vaporization, correlation laws are used both for heat and mass transfer modifications under the film theory assumption. Following Faeth [15], Nusselt number is then expressed through:

$$Nu = Nu^* \ln(1 + B_T) \text{ and } Nu^*$$

$$= 2 + \frac{0.55 Re^{1/2} Pr^{1/3}}{\left(1 + \frac{1.232}{Re Pr^{4/3}}\right)^{1/2}} \quad (7)$$

where B_T is the Spalding heat transfer number, Re is the particle Reynolds number and Pr is the Prandtl number. A similar relation is written for the Sherwood number, but with the Prandtl number replaced by the Schmidt number.

An important issue in evaluating the droplet vaporization rate is the knowledge of the physical properties in the gaseous film around the droplet. Following Hubbard *et al.* [16], the averaging “1/3 rule” should be used, namely physical properties of the fluid around the particle have to be approximated at a reference state “1/3 of the droplet surface + 2/3 of the fluid far from the droplet”. That leads to the change in the drag coefficient C_D through the viscosity ν in the particle Reynolds number which is now calculated at the reference state (v_{ref} in equation 10). We have observed a quite large sensitivity of the droplet behaviour to a modification of that rule (Berlemont *et al.* [9]).

PARTICLE TRACKING

Due to the quite large particle and fluid density ratio, forces in the droplet motion equation are reduced to drag and gravity forces, leading to:

$$\rho_1 \frac{\pi D^3}{6} \frac{d\mathbf{V}}{dt} = -\frac{\pi D^2}{8} \rho C_D (\mathbf{V} - \mathbf{U}) |\mathbf{V} - \mathbf{U}| + \frac{\pi D^3}{6} (\rho_1 - \rho) g \quad (8)$$

with following Clift *et al.* [17]:

$$C_D = \frac{24}{Re_p} (1 + 0.15 Re_p^{0.687}) \quad (9)$$

where the particle Reynolds number Re_p is defined as:

$$Re_p = \frac{|\mathbf{V} - \mathbf{U}| D}{\nu_{\text{ref}}} \quad (10)$$

Re_p is assumed to be smaller than 200. \mathbf{V} and \mathbf{U} are the droplet and fluid velocity vectors respectively, and g is the acceleration due to gravity.

The main problem arising in the integration of the equation of motion of a discrete particle is to determine the instantaneous fluid velocity at the location of the discrete particle. That problem is the basis of the different schemes which are used in Lagrangian approaches (Gosman and Ioannides [18], Durst *et al.* [19], Sommerfeld [20], Azevedo and Pereira [21], Berlemont *et al.* [22]). Mean velocities are obtained through any kind of turbulence model, but fluid velocity fluctuations can be determined through different random schemes.

In our approach (Berlemont *et al.* [9], [22]) the random process can be driven by given correlation functions. Rather than using a stochastic process leading to a fixed Lagrangian velocity correlation function, we choose this function and slave the random process to it. This is achieved through a correlation matrix (Berlemont *et al.* [23]) implementing the chosen velocity correlation function. In practice we privileged Frenkiel [24] correlations which involve a loop parameter driving the occurrence and importance of negative loops in the correlation. However, the most important problem in particle tracking process remains the turbulent scale approximations as recently discussed (Berlemont *et al.* [1]). In both Lagrangian integral time scale and Eulerian length scale a constant has to be set. It has been shown that particle dispersion is very sensitive to the value of these constants. Examples may be found in Gouesbet *et al.* [25].

TWO-WAY COUPLING

When vaporizing droplets are involved in the simulations, two-way coupling must be accounted for since the phase change modifies the characteristics of the fluid phase. The vapour produced by the droplets is a mass source for the fluid, moreover the vaporization process generates modifications in the momentum and energy balances between both phases. Fluid phase equations then contain many extra-source terms. Assuming that the vapour production does not significantly modify the fluid phase density, the governing equations read as follows (Grancher [26]), with classical notations:

Mean flow equations

Continuity equation:

$$\frac{\partial}{\partial x_i} (\rho U_i) = \mathcal{S}_m \quad (11)$$

where \mathcal{S}_m is the mass source term.

Momentum equation:

$$\frac{\partial}{\partial x_j} (\rho \bar{U}_i \bar{U}_j) = -\frac{\partial}{\partial x_i} [\bar{P} + \frac{2}{3} \rho k] - \frac{\partial}{\partial x_i} \left[\frac{2}{3} (\mu + \mu_T) \frac{\partial \bar{U}_j}{\partial x_j} \right] + \frac{\partial}{\partial x_j} (\mu + \mu_T) \left(\frac{\partial \bar{U}_i}{\partial x_j} + \frac{\partial \bar{U}_j}{\partial x_i} \right) + \bar{S}_{u_i} \quad (12)$$

where S_{u_i} is the momentum source term, which involves two terms associated with two phenomena: $\bar{S}_{u_i} = \bar{S}_{pu_i} + \bar{S}_{mu_i} - \bar{S}_{pv_i}$ is linked to interaction forces between the fluid and the particles:

$$\bar{S}_{pv_i} = n \left\langle -m_p \left(\frac{dV_i}{dt} - g_i \right) \right\rangle \quad (13)$$

where n is the mean number of particles per unit volume.

$-\bar{S}_{mu_i}$ is the gas momentum flux ejected by the particle during its vaporization. Assuming that the vapour is discharged into the fluid with a mean velocity nearly equal to the droplet velocity, we get:

$$\bar{S}_{mu_i} = n \langle S_m V_i \rangle. \quad (14)$$

Mean temperature:

$$\frac{\partial}{\partial x_j} (\rho \bar{U}_j \bar{T}) = \frac{\partial}{\partial x_j} \left(\frac{\mu}{Pr} + \frac{\mu_T}{Pr_T} \right) \left(\frac{\partial \bar{T}}{\partial x_j} \right) + \bar{S}_H / C_p \quad (15)$$

where \bar{T} is the mean temperature defined with respect to a reference temperature T_{ref} , S_H is the enthalpy source term and C_p is the fluid specific heat capacity S_H can be divided in two parts:

$-\bar{S}_{pH}$ which represents the heat captured by the droplet for its heating and for vaporizing \dot{m} mass of liquid per unit time:

$$\bar{S}_{pH} = n \langle -4\pi r_s^2 q_g \rangle. \quad (16)$$

$-\bar{S}_{mH}$ which represents the heat which is released by the droplet into the fluid:

$$\bar{S}_{mH} = n \langle \dot{m} C_{vap} (T_s - T_{ref}) \rangle. \quad (17)$$

Mean vapour mass fraction:

$$\frac{\partial}{\partial x_j} (\rho \bar{U}_j \bar{Y}) = \frac{\partial}{\partial x_j} \left(\frac{\mu}{Sc} + \frac{\mu_T}{Sc_T} \right) \left(\frac{\partial \bar{Y}}{\partial x_j} \right) + \bar{S}_m \quad (18)$$

where Sc and Sc_T are the Schmidt number and turbulent Schmidt number, respectively.

Turbulence equations

Fluid turbulence is still described using a $(k-\varepsilon)$ model, but the modification of the continuity equation leads to extra terms in the k -equation, ε -equation and for temperature and vapour mass fraction fluctuation equations.

Turbulence energy equation. Applying the Reynolds decomposition to the momentum equation, we first obtain:

$$\begin{aligned} \frac{\partial}{\partial t} \rho u'_i + \frac{\partial}{\partial x_j} \rho [\bar{U}_j u'_i + \bar{U}_j u'_j + u'_i u'_j - \overline{u'_i u'_j}] \\ = -\frac{\partial p'}{\partial x_i} - \frac{\partial}{\partial x_i} \left[\frac{2}{3} \mu \frac{\partial u'_k}{\partial x_k} \right] + \frac{\partial}{\partial x_j} 2\mu s'_{ij} + S'_{u_i} \end{aligned} \quad (19)$$

where

$$s'_{ij} = \frac{1}{2} \left(\frac{\partial u'_i}{\partial x_j} + \frac{\partial u'_j}{\partial x_i} \right)$$

is the fluctuating part of the strain tensor.

Multiplying (19) by u'_i , summing on subscript i and averaging, we obtain:

$$\begin{aligned} \frac{\partial}{\partial x_j} [\rho \bar{U}_j k + \frac{1}{2} \rho \overline{u'_i u'_i u'_i} - 2\mu \overline{u'_i s'_{ij}} + \overline{p' u'_j}] \\ = -\rho \overline{u'_i u'_j} \bar{S}_{ij} - 2\mu \overline{s'_{ij} s'_{ij}} \quad (I) \\ + \overline{S'_{u_i} u'_i} \quad (II) \\ - \rho k \frac{\partial \bar{U}_k}{\partial x_k} - \left(\frac{2}{3} \overline{u'_i \frac{\partial}{\partial x_i} \mu \frac{\partial u'_k}{\partial x_k}} \right) - \frac{1}{2} \overline{\rho u'_i u'_i \frac{\partial u'_k}{\partial x_k}} \\ + \overline{p' \frac{\partial u'_k}{\partial x_k}} - \rho \overline{U_i u'_i \frac{\partial u'_k}{\partial x_k}} \quad (III). \end{aligned} \quad (20)$$

Part (I) of the above equation is the usual turbulence energy equation (Tenneskes and Lumley [27]), part (II) is linked to the fluctuations of the momentum source term and part (III) is only generated by the phase changes. Term (III) is now detailed.

Using equation (11), and neglecting density fluctuations such as $\partial u'_k / \partial x_k = S'_m \rho$, we get:

$$\begin{aligned} (III) = -k \bar{S}_m - \frac{1}{2} \overline{u'_i u'_i S'_m} - \overline{U_i u'_i S'_m} \\ (1) \quad (2) \quad (3) \\ - \frac{2}{3} \frac{\mu}{\rho} \overline{u'_i \frac{\partial S'_m}{\partial x_i}} + \frac{1}{\rho} \overline{p' S'_m}. \end{aligned} \quad (21)$$

The term (1) depends on the mean mass source term, when other terms depend on the fluctuations of this mean mass source term. The terms (2) and (3) can be directly obtained without any assumption since we are concerned, here, with a Lagrangian approach, but the terms (4) and (5) should be modelled. However, it appears to be reasonable to neglect the correlation between velocity fluctuations and spatial derivative of mass source term fluctuations (term 4) and between pressure fluctuations and mass source term fluctuations (term 5). Equation (20) thus reads:

$$\frac{\partial}{\partial x_j} (\rho \bar{U}_j k) = \frac{\partial}{\partial x_j} \left(\frac{\mu_T}{\sigma_k} \right) \left(\frac{\partial k}{\partial x_j} \right) + \mathcal{S}_k \quad (22)$$

$$\mathcal{S}_k = G - C_D \rho \varepsilon + S_k \quad (23)$$

where

$$G = \mu_T \left[\frac{\partial \bar{U}_i}{\partial x_j} + \frac{\partial \bar{U}_j}{\partial x_i} \right] \frac{\partial \bar{U}_i}{\partial x_j}$$

is the usual turbulence energy production term, and

S_k is the extra source term which can be separated in two parts:

$$S_k = S_{pk} + S_{mk} \quad (24)$$

where S_{pk} is linked to the particle mass loading:

$$S_{pk} = \overline{S'_{pu_i} u'_i} \quad (25)$$

and S_{mk} is due to the vaporization process:

$$\begin{aligned} S_{mk} &= \overline{S'_{mu_i} u'_i} - k \overline{S_m} - \frac{1}{2} \overline{u'_i u'_i S'_m} - \overline{U_i u'_i S'_m} \\ &= \overline{S'_{mu_i} u'_i} + \frac{1}{2} \overline{U_i U_i S'_m} - \frac{1}{2} \overline{U_i U_i S'_m}. \end{aligned} \quad (26)$$

Energy dissipation rate equation. The same model is used for particle source term in ε -equation with and without vaporization, that means extra dissipation due to the particles is assumed to be proportional to their energy production:

$$S_{pe} = C_{e3} \frac{\varepsilon}{k} S_{pk}. \quad (27)$$

The transport equation thus reads:

$$\frac{\partial}{\partial x_j} (\rho \overline{U_j \varepsilon}) = \frac{\partial}{\partial x_j} \left(\frac{\mu_T}{\sigma_\varepsilon} \right) \left(\frac{\partial \varepsilon}{\partial x_j} \right) + \mathcal{S}_\varepsilon \quad (28)$$

with

$$\mathcal{S}_\varepsilon = C_1 \frac{\varepsilon}{k} G - C_2 \rho \frac{\varepsilon^2}{k} + S_\varepsilon \quad \text{and}$$

$$S_\varepsilon = C_{e3} \frac{\varepsilon}{k} (S_{pk} + S_{mk}). \quad (29)$$

Scalar fluctuation transport equation. Scalar fluctuation transport equation is obtained by deriving the transport equation for a scalar fluctuation. By multiplying the transport equation for θ' by θ' , by

averaging and by assuming that $\partial \rho U_i / \partial x_i = S_m$ and $\partial \rho u'_i / \partial x_i = S'_m$, we can write:

$$\frac{\partial}{\partial x_j} (\rho \overline{U_j \theta'^2}) = \frac{\partial}{\partial x_j} \left(\frac{\mu_T}{\sigma_\theta} \right) \left(\frac{\partial \theta'^2}{\partial x_j} \right) + \mathcal{S}_\theta \quad (30)$$

with

$$\mathcal{S}_\theta = C_{\theta 1} \mu_T \frac{\partial \overline{\theta}}{\partial x_j} \frac{\partial \overline{\theta}}{\partial x_j} - C_{\theta 2} \rho \frac{\varepsilon}{k} \overline{\theta'^2} + S_\theta \quad (31)$$

and

$$\begin{aligned} S_\theta &= \overline{S'_\theta \theta'} - \overline{\theta'^2 S'_m} - \overline{\theta'^2 S'_m} - 2 \overline{\theta' \theta' S'_m} \\ &= \overline{S'_\theta \theta'} + \overline{\theta \theta' S'_m} - \overline{\theta \theta' S'_m}. \end{aligned} \quad (32)$$

All the source terms are summarized in Table 1.

TWO PHASE VAPORIZING DROPLET JET SIMULATION

Experiments on evaporating sprays which can be used for model validation are needed; however they are very rare due to the complexity of measurements required for comparisons. For the model validation such experiments should provide us with detailed inlet conditions, and in particular droplet size velocity correlations. Since at this time no experiment was found for our purpose, we have decided to simulate the turbulent round particle laden jet configuration which is now described.

Test case description

We arbitrary chose a physical problem, such as the influence of the discrete phase on the carrier fluid

Table 1. Source terms in turbulence model

Φ	Continuity equation: $\frac{\partial}{\partial x_j} \rho \overline{U_j} = \overline{S_m}$	
	$\overline{S_\Phi}$ (turbulence model)	$\overline{S_\Phi} = \overline{S_{p\Phi}} + \overline{S_{m\Phi}}$ (extra source terms)
U_i	$-\frac{\partial}{\partial x_i} (P + \frac{2}{3}k) - \frac{\partial}{\partial x_i} \frac{2}{3} \mu_t \frac{\partial \overline{U_j}}{\partial x_j} + \overline{S_{U_i}}$	$S_{pU_i} = n \left\langle -m_p \left[\frac{dV_i}{dt} - g_i \right] \right\rangle$ $S_{mU_i} = n \langle S_m V_i \rangle$
k	$G - C_D \rho \varepsilon + S_k$	$S_{pk} = \overline{S'_{pu_i} u'_i}$ $S_{mk} = \overline{S'_{mu_i} u'_i} + \frac{1}{2} \overline{U_i U_i S'_m} - \frac{1}{2} \overline{U_i U_i S'_m}$
ε	$C_1 \frac{\varepsilon}{k} G - C_2 \rho \frac{\varepsilon^2}{k} + S_\varepsilon$	$S_\varepsilon = C_{e3} \frac{\varepsilon}{k} S_k$
$c_p T$	S_H	$S_{pH} = -n \langle L \dot{m} + Q_L \rangle$ $S_{mH} = n \langle \dot{m} C_{vap} (T_s - T_0) \rangle$
Y	S_m	$S_m = n \langle \dot{m} \rangle$
θ'^2	$C_{\theta 1} \mu_t \frac{\partial \overline{\theta}}{\partial x_j} \frac{\partial \overline{\theta}}{\partial x_j} - C_{\theta 2} \rho \frac{\varepsilon}{k} \overline{\theta'^2} + S_\theta$	$S_\theta = \overline{S'_\theta \theta'} + \overline{\theta \theta' S'_m} - \overline{\theta \theta' S'_m}$

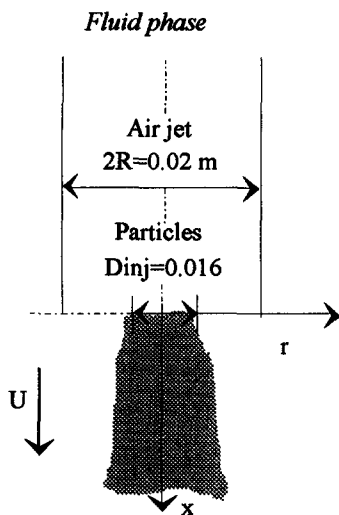


Fig. 1. Simulation test case.

should be quite important. We thus assumed a high mass loading ratio, namely $\Phi = 0.5$, and the droplet inlet velocity was taken smaller than the fluid velocity in order to increase the vapour production (which increases when the droplet relative velocity increases).

We consider a turbulent round jet vertically aligned with the main direction set downward (Fig. 1). Jet exit diameter is 0.02 m, and centerline exit mean velocity is 28 m s^{-1} . Initial profiles for mean velocities and turbulence are deduced from fully developed pipe flow predictions. Mean temperature is 400 K, and is assumed constant everywhere in the jet. No temperature fluctuations are introduced into the flow field.

Droplet characteristics. Methyl-alcohol droplets are injected at the jet exit, from $r = 0 \text{ m}$, to $r = 0.008 \text{ m}$. Initial diameter is $100 \mu\text{m}$, and the initial droplet temperature is 300 K. Droplet injection velocity is 0.7 times the fluid velocity. Fluid and particle initial velocity fluctuations are identical.

Fluid phase predictions. Fluid flow calculations are carried out by using a $(k-\epsilon)$ model supplemented with algebraic relations, deduced from second order closure assumption, for the Reynolds tensor prediction (Gosman *et al.* [28], Rodi [29]). Cylindrical coordinates are used with (80×40) grid nodes.

Constants. Classic correction for turbulent round jet predictions is used, namely:

$$C_\mu = 0.09 - 0.04f \quad C_2 = 1.92 - 0.067f$$

with

$$f = \left[\frac{r_{1/2}}{2\Delta U} \left(\frac{\partial U_{c1}}{\partial x} - \left| \frac{\partial U_{c1}}{\partial x} \right| \right) \right]^{0.2} \quad (33)$$

where U_{c1} is the longitudinal centerline mean velocity, $r_{1/2}$ is the jet half-width and ΔU the longitudinal mean velocity radial variation on $r_{1/2}$. Other constants are:

$$C_D = 1, \quad C_1 = 1.44, \quad \sigma_k = 1.0,$$

$$\sigma_\epsilon = 1.3 \quad \text{and} \quad C_{\epsilon_3} = 1.1.$$

Droplet statistics are carried out on 20000 trajectories and eight iterations are made between turbulence prediction and droplet trajectory simulations.

RESULTS

Uniform temperature field

Discussion is first carried out by only considering mass, momentum and energy source terms. Heat source terms will be introduced in the next section.

Figure 2 presents reduced mean centerline velocity profiles (U_{c1}/U_0) for the single phase, for the fluid phase with $\Phi = 0.5$ and for the droplets (U_0 is the fluid jet exit velocity), vs $x/2R$. Up to $x/2R = 10$, the droplets are accelerating and due to their lower velocity than the fluid flow, they slightly decrease the fluid velocity. When $x/2R$ is greater than 10 the fluid velocity is increased by the droplets, but the gap between particle and fluid velocities is decreasing due to the droplet vaporization, also inducing less particle influence on the fluid flow. We can observe in Fig. 3 that the jet half width is decreased as observed too in particle laden jets (Berlemont *et al.* [22]), but the decrease of the droplet mass flow rate leads to an increase in the slope of the jet half width profile which tends back to the single phase flow case.

Reduced droplet diameters on the jet axis are presented in Fig. 4. We observe for $x/2R > 10$ that the decrease in diameter is smaller with the two-way coupling than the simulations without iteration between the turbulent field and the particles. This result can be explained by the increase of the fluid velocity and thus of the droplet velocity, which leads to a shorter droplet residence time in the simulation domain.

Figure 5 shows the centerline vapour mass fraction induced by the droplet vaporization. We can first observe a clear decrease in vapour mass fraction near $x/2R = 10$ which can be explained by two mechanisms. First as the particle velocity equals the fluid velocity in that region, vapour production decreases due to reduction of the convection flux proportionally to the particle relative velocity. Secondly, as shown in Fig. 6, the turbulent energy is highly increased near $x/2R = 10$, thus the turbulent diffusion is greater than production in that region. These mechanisms processes are then inverted near $x/2R = 15$ until $x/2R = 55$. In this region the droplet diameters are decreased due to vaporization and the turbulent dispersion drives the particle towards the edges of the jet; consequently the vapour production is decreased on the axis.

The axial turbulence intensity on the jet axis is presented in Fig. 6. The single phase value is stabilized around 27%, and a classical turbulent intensity decrease, due to the presence of particles, is observed for the two phase flow. As previously mentioned for the velocities, the influence of the particles on the fluid

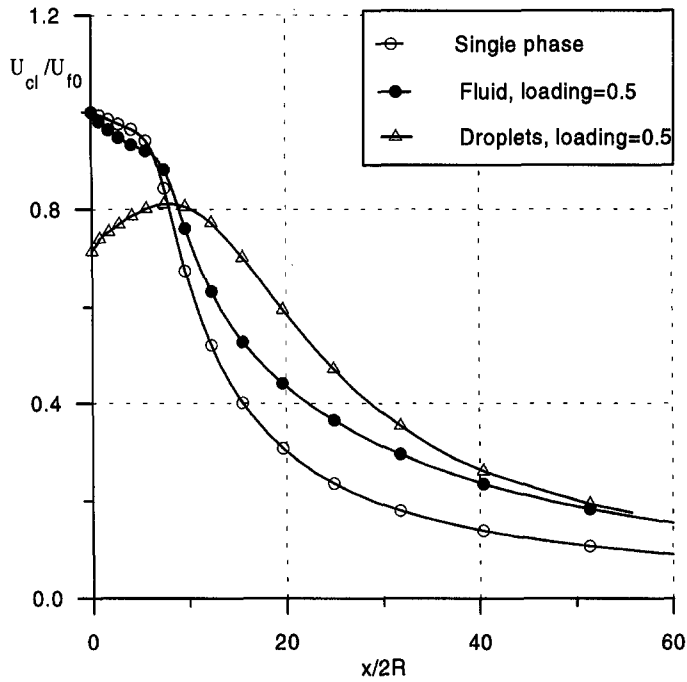


Fig. 2. Reduced centerline mean velocities.

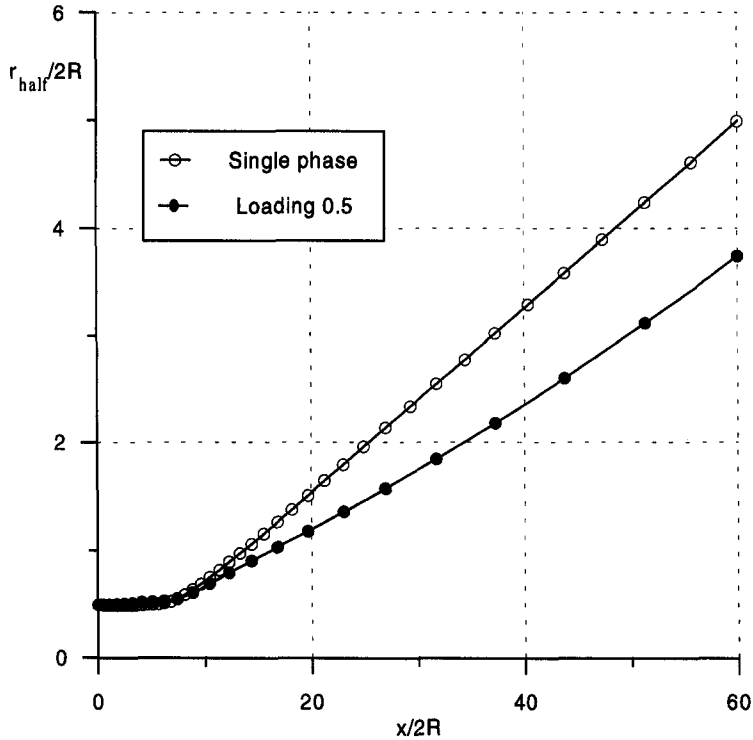


Fig. 3. Reduced jet half width.

is decreased during the droplet vaporization process. As described in Table 1, the source terms are divided in two parts, one coming from the mere presence of the droplet and the second one which is linked to the droplet vaporization process. Figure 7 represents an estimate of the contribution of each part. By com-

paring these two terms it can be observed that the vaporization source term is much smaller (in absolute value) than the usual source term for two way coupling on the turbulent energy equation.

Droplet mean diameters and rms diameter are presented in Figs 8 and 9, respectively. The profiles are

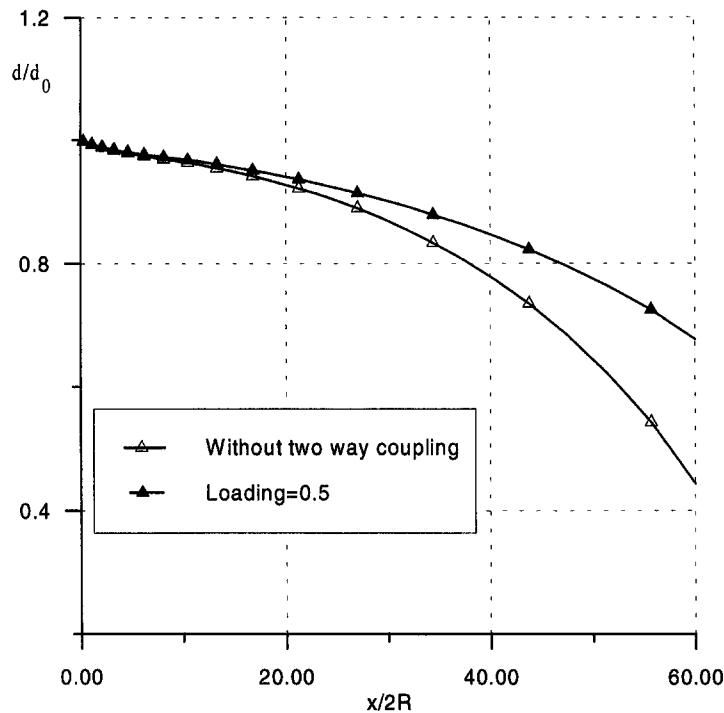


Fig. 4. Droplet diameter on jet axis.

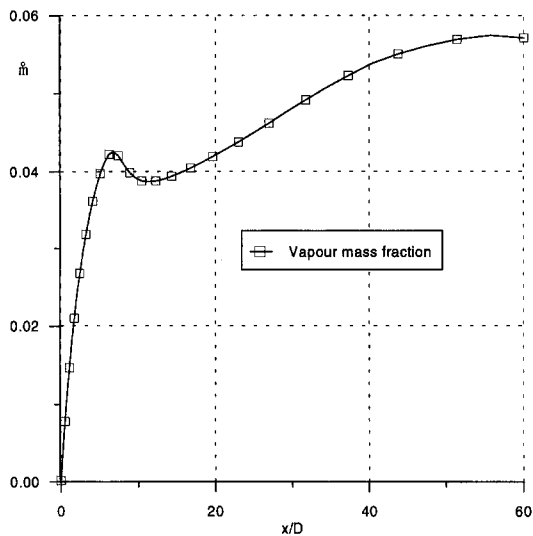


Fig. 5. Vapour mass fraction.

reduced by the initial droplet diameter ($100 \mu\text{m}$). In these figures we observe that the smaller droplets are present on the jet edges, and this behaviour is more pronounced as they move downstream the jet exit. Moreover, the droplet diameter standard deviation is increasing from the jet axis to the edge: for example, at the location $x/2R = 120$, σ_d is equal to $5 \mu\text{m}$ and $d = 68 \mu\text{m}$ on the axis, since $\sigma_d = 10 \mu\text{m}$ and $d = 55 \mu\text{m}$ for $r/R = 4$. Statistics on the outer part of the jet are computed on roughly 200 droplets, a quite small number but which is sufficient to point out a physical behaviour. It is worth pointing that the droplets en-

countered on the edge of the jet can exhibit different histories: they can be on the jet edge since their injection and thus their quite long residence time in the jet leads to a small diameter, or they can travel from the jet axis to the edge by dispersion effect and thus they keep a larger diameter.

Fluid temperature modifications

In the above discussion, the fluid temperature has been assumed constant. This section presents the same simulation but this time the two way coupling is now introduced in the fluid temperature predictions as defined in Table 1.

Figure 10 presents the droplet mean diameter on the jet axis with and without coupling on temperatures. We observe that the droplet diameter is decreasing more slowly with temperature two way coupling than without. That behaviour can be explained by drawing the fluid temperature on the jet axis (Fig. 11). A quite fast decrease of the temperature is observed near the jet exit. That behaviour is linked to the droplet injection conditions: since the droplet slip velocities are quite important, convection phenomena induce more intense heat transfers between both phases, as previously mentioned in the discussion of Fig. 5. Then the mean temperature is increased by turbulent diffusion which induces energy transfers from the jet edge (where the temperature is fixed to 400 K) to the axis. We then observe a slight decrease of the jet axis temperature which represents the gap between the turbulent heat diffusion and the absorbed heat through droplet vaporization.

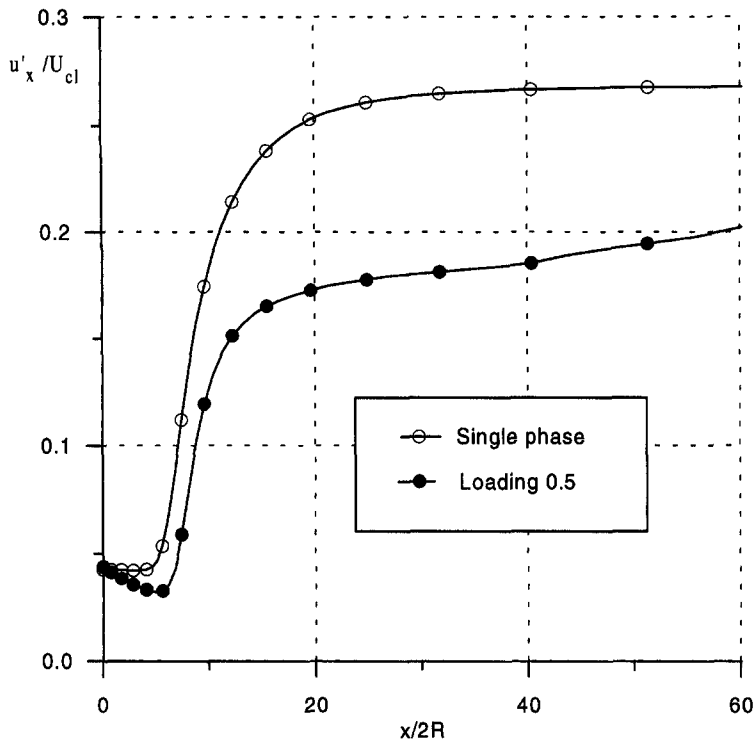
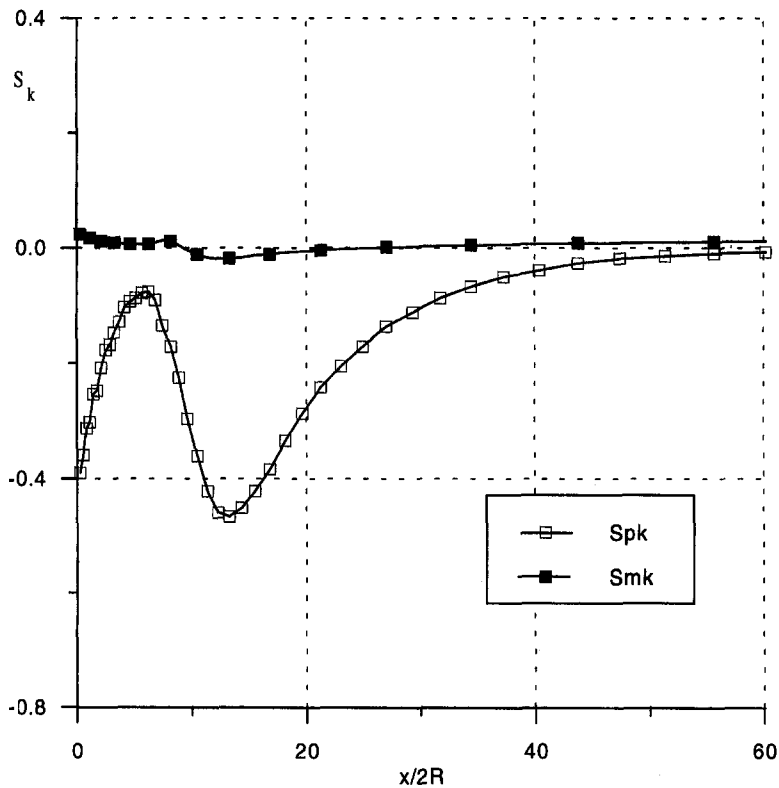


Fig. 6. Jet axis longitudinal turbulence intensity.

Fig. 7. Comparison of source terms in the k -equation.

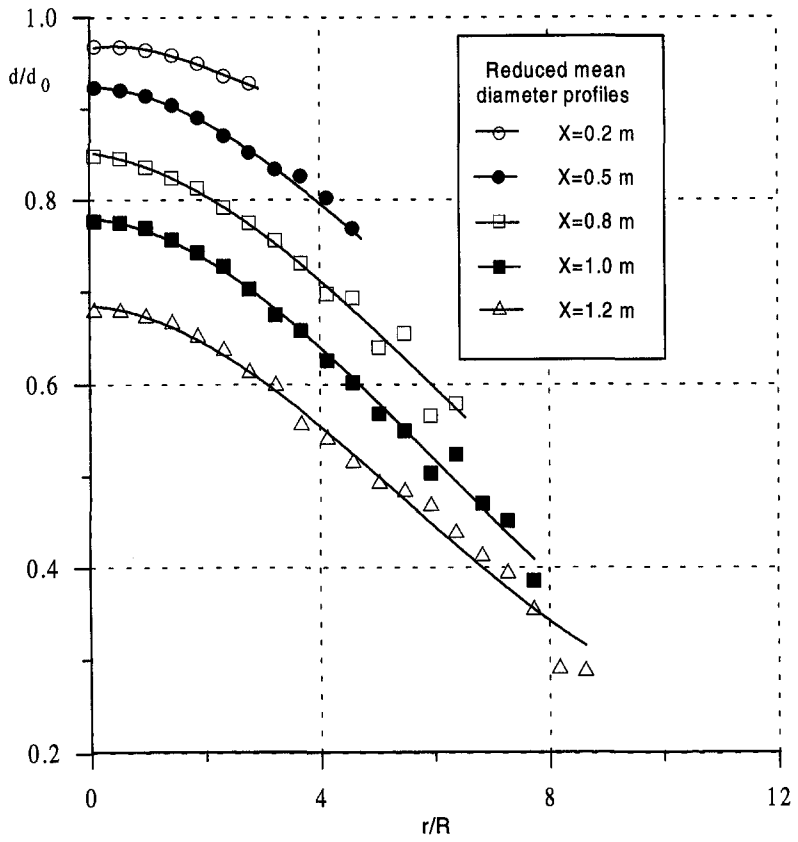


Fig. 8. Droplet diameter profiles.

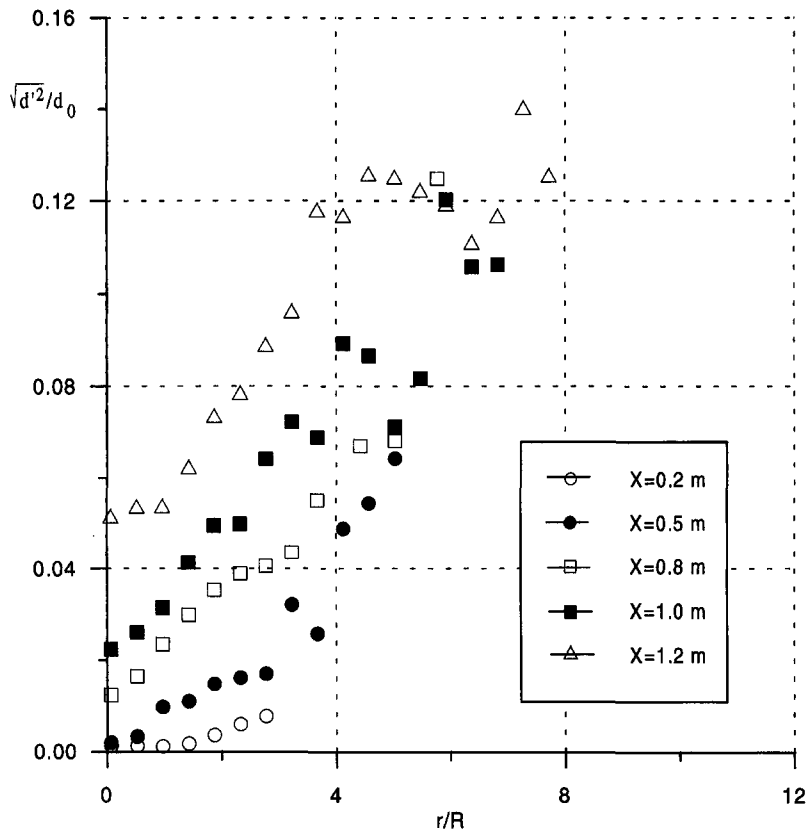


Fig. 9. Droplet diameter rms profiles.

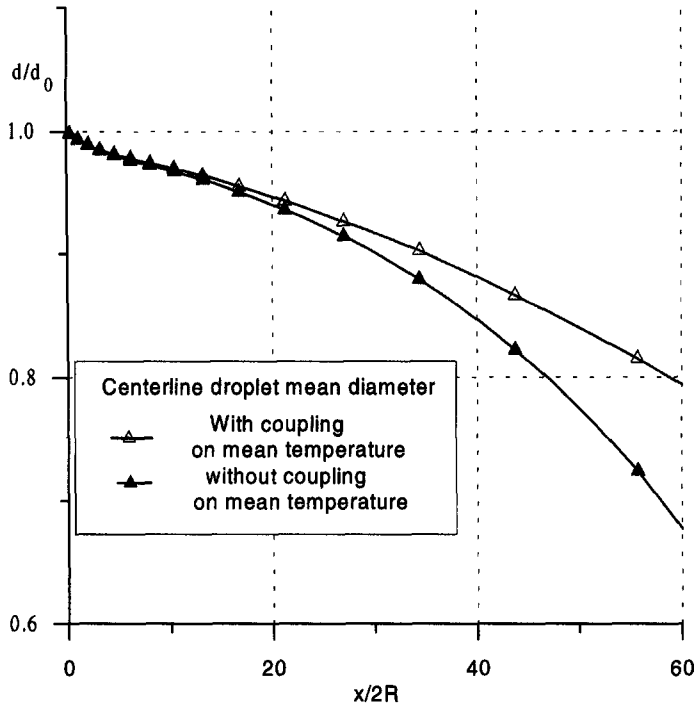


Fig. 10. Droplet diameter on jet axis.

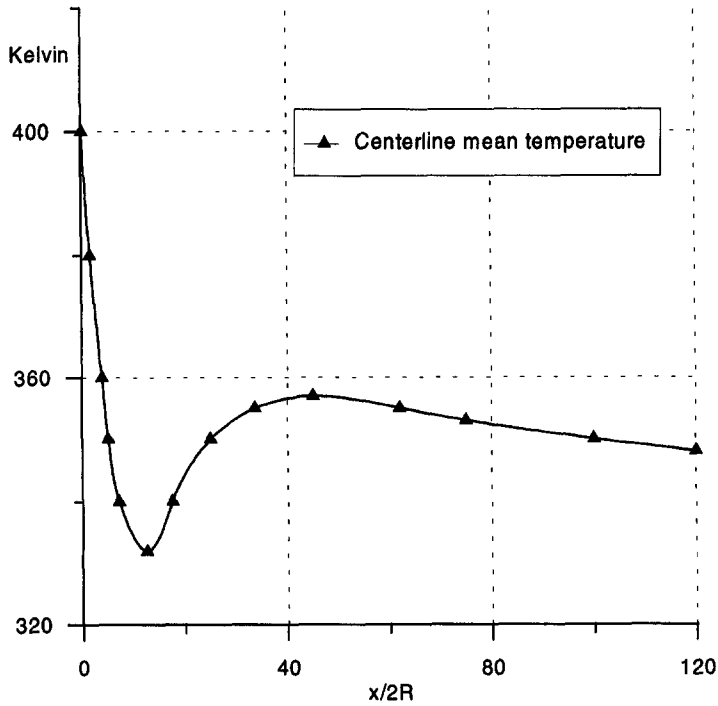


Fig. 11. Mean temperature on jet axis.

CONCLUSION

Two-way coupling between gas phase and liquid phase has been presented for the study of vaporizing droplets in turbulent round jets. Following the well recognized scheme to model the influence of discrete particles on turbulence field for high mass loading flows, we have established the source terms linked to the vaporization process. These source terms appear in the continuity, momentum, turbulence energy, turbulent dissipation, temperature and vapour mass fraction transport equations. Using a Lagrangian approach, all the terms are exact, except for the turbulent energy dissipation rate which is modeled.

We have then carried out simulations for methyl alcohol droplet vaporization in a heated turbulent round jet to determine the interaction dispersion-vaporization and the strong coupling between the two phases. In the studied case, we have observed that the influence of the droplets on the fluid turbulent energy is mainly due to the presence of the particles, rather than the extra source term coming from the vaporization process. We have mentioned that the turbulence leads to quite large diameter distributions on the jet edges. Moreover, a high coupling is observed between production and turbulent diffusion, both at the vapour mass fraction and fluid temperature levels. Finally, we have observed that our two way coupling method needs more iterations between the turbulence transport and the droplet trajectories equation. This is due to the required precision on the fluid flow which drives the history of the droplet dynamics (residence time and temperatures which are encountered). The next step in our studies will be to confirm the presented results by comparing simulations and experimental results as soon as detailed experiments will be available.

REFERENCES

1. A. Berlemont, P. Desjonquères and G. Gouesbet, Particle tracking in turbulent flows, *Proceedings of the ASME Gas-Solid Flows Conference*, Washington, DC, 20-24 June, ASME-FED Vol. 166, pp. 121-131 (1993).
2. M. W. Reeks, On the dispersion of small particles suspended in an isotropic turbulent fluid, *J. Fluid Mech.* **83**, 529-546 (1977).
3. S. E. Elghobashi, T. W. Abou Arab, M. Rizk and A. Mostafa, Prediction of the particle laden jet with a two equation turbulence model, *Int. J. Multiphase Flow* **10**, 697-710 (1984).
4. A. Picart, A. Berlemont and G. Gouesbet, Modelling and predicting turbulence fields and dispersion of discrete particles transported by turbulent flows, *Int. J. Multiphase Flow* **12**, 237-261 (1986).
5. G. Gouesbet, A. Berlemont and A. Picart, Dispersion of discrete particles by turbulent continuous motions. extensive discussion of Tchen's theory using a two parameter family of Lagrangian correlation functions, *Phys. Fluids* **27**, 827-837 (1984).
6. P. Desjonquères, G. Gouesbet, A. Berlemont and A. Picart, Dispersion of discrete particles by continuous turbulent motions: new results and discussions, *Phys. Fluids* **29**, 2147-2151 (1986).
7. O. Simonin, Prediction of the dispersed phase turbulence in particle laden jets, *Proceedings ASME Gas-Solid Flows Conference*, Washington, DC, 20-24 June, ASME-FED Vol. 121, pp. 197-206 (1991).
8. M. W. Reeks, On the constitutive relations for dispersed particles in non uniform flows, *Phys. Fluids A* **5**(3), 750-761 (1993).
9. A. Berlemont, M. S. Grancher and G. Gouesbet, On the Lagrangian simulation of turbulence influence on droplet evaporation, *Int. J. Heat Mass Transfer* **34**(11), 2805-2812 (1991).
10. D. B. Spalding, *Combustion and Mass Transfer*. Pergamon Press, Oxford (1979).
11. A. Linan, Theory of Droplet Vaporisation and Combustion, Ecole d'été sur les Problèmes non linéaires Appliqués, Lecture in CEA-INRIA-EDF (1985).
12. S. Prakash and W. A. Sirignano, Theory of convective droplet vaporisation with unsteady heat transfer in the circulation liquid phase, *Int. J. Heat Mass Transfer* **23**, 253-268 (1980).
13. S. K. Aggarwal, A. Y. Tong and W. A. Sirignano, A comparison of vaporization models in spray combustion, *AIAA J.* **22**, 10 (1984).
14. M. Renksizbulut and R. J. Haywood, Transient droplet evaporation with variable properties in an internal circulation at intermediate Reynolds numbers, *Int. J. Multiphase Flow* **14**(2), 189-202 (1988).
15. G. M. Faeth, Current status of droplet and liquid combustion, *Prog. Energy Combustion Sci.* **3**, 191-224 (1977).
16. G. L. Hubbard, V. E. Denny and A. F. Mills, Droplet evaporation: effects of transient and variable properties, *Int. J. Heat Mass Transfer* **18**, 1003-1008 (1975).
17. R. Clift, J. R. Grace and M. E. Weber, *Bubbles, Drops and Particles*. Academic Press, New York (1978).
18. A. D. Gosman and E. Ioannides, Aspects of computers simulation of liquid-fuelled combustors, Presented at the *AIAA 19th Aerospace Science Meeting*, St Louis, MO, Paper 81-0323 (1981).
19. F. Durst, D. Milojevic and B. Schonung, Eulerian and Lagrangian predictions of particulate two-phase flows: a numerical study, *Appl. math. Modelling* **8**, 101-115 (1984).
20. M. Sommerfeld, Numerical simulation of the particle dispersion in turbulent flow: the importance of lift forces and particle-wall collision models, *Numerical Methods for Multiphase Flows*, ASME-FED Vol. 91, pp. 11-18 (1990).
21. J. L. T. Azevedo and J. C. F. Pereira, Prediction of gas-particle turbulent free and confined flows, Part. *Part. Systems Characterization* **7**, 171-180 (1991).
22. A. Berlemont, P. Desjonquères and G. Gouesbet, Particle Lagrangian simulation in turbulent flows, *Int. J. Multiphase Flow* **16**(1), 19-34 (1990).
23. A. Berlemont, G. Gouesbet and P. Desjonquères, Lagrangian simulation of particle dispersion, Proc. United States-France Joint Workshop on Turbulent Reactive Flows, Rouen, 6-10 July, *Lecture Notes in Engineering*, 40. Springer, Berlin (1987).
24. F. N. Frenkiel, Etude statistique de la turbulence-fonctions spectrales et coefficients de corrélation, Rapport Technique, ONERA no. 34 (1948).
25. G. Gouesbet, A. Berlemont, P. Desjonquères and G. Gréhan, On modelling and measurement problems in the study of turbulent two-phase flows with particles, *Proceedings of the 6th Workshop on Two Phase Flow Prediction*, pp. 365-387 (Edited by Sommerfeld). Erlangen, Germany (1992).
26. M. S. Grancher, Simulation de l'évaporation de gouttelettes en écoulement turbulent suivant une approche lagrangienne, Thèse de Doctorat, Université de Rouen (1990).
27. H. Tennekes and J. Lumley, *A First Course in Turbulence*. MIT Press, Cambridge, MA (1974).
28. A. D. Gosman and F. J. K. Ideriah, *Teach T Manual*, Department of Mechanical Engineering, Imperial College of Sciences and Technology, London (1976).
29. W. Rodi, *Turbulence Models for Environmental Problems*, VKI Lectures Series 2979-2, (1979).